

Geometry of Spatial Memory Replay

Y. Dabaghian

*Jan and Dan Duncan Neurological Research Institute,
Baylor College of Medicine, Houston, TX 77030,
and the Department of Computational and Applied Mathematics,
Rice University, Houston, TX 77005*

e-mail: dabaghia@bcm.edu

(Dated: April 25, 2022)

Place cells in the rat hippocampus play a key role in creating the animal's internal representation of the world. During active navigation, these cells spike only in discrete locations, together encoding a map of the environment. Electrophysiological recordings have shown that the animal can revisit this map mentally, during both sleep and awake states, reactivating the place cells that fired during its exploration in the same sequence they were originally activated. Although consistency of place cell activity during active navigation is arguably enforced by sensory and proprioceptive inputs, it remains unclear how a consistent representation of space can be maintained during spontaneous replay. We propose a model that can account for this phenomenon and suggests that a spatially consistent replay requires a number of constraints on the hippocampal network that affect its synaptic architecture and the statistics of synaptic connection strengths.

I. INTRODUCTION

In the course of learning a spatial environment, an animal forms an internal representation of space that enables spatial navigation and planning [1]. The hippocampus plays a key role in producing this map through the activity of location-specific place cells [2]. At the neurophysiological level, these place cells exhibit spatially selective spiking activity. As the animal navigates its environment, the place cell fires only at a discrete location—its place field (Figure 1A-B). It is believed that the entire ensemble of place cells serves as a neuronal basis of the animal’s spatial awareness [3, 4].

Remarkably, place cells spike not only during active navigation but also during quiescent wake states [5, 6] and even during sleep [7–9]. For example, the animal can “replay” place cells in sequences that correspond to the physical routes traversed during active navigation [10–12] or “preplay” sequences that represent possible future trajectories, either in direct or reversed order, while pausing at a decision point [14, 15]. This phenomenon implies that, after learning, the animal can explore and retrieve spatial information by cuing the hippocampal network [16, 17], which may in turn be viewed as a physiological correlate of “mental exploration” [18, 19].

It bears noting, however, that the actual functional units for spatial information processing in the hippocampal network are not individual cells but repeatedly activated groups of place cells known as cell assemblies (see [20] and Figure 1C). Although the physiological properties of the place cell assemblies remain largely unknown, it is believed that the cells constituting an assembly synaptically drive a certain readout unit downstream from the hippocampus. In the “reader-centric” view, this readout neuron—a small network or, most likely, a single neuron—is what actually defines the cell assembly, by actualizing the information provided by its activity [20]. The identity of the readout neurons in some cases is suggested by the network’s anatomy. For example, there are direct many-to-one projections from the CA3 region of the hippocampus to the CA1 region. Since replays are believed to be initiated in CA3 [13, 14], this implies that the CA1 place cells may serve as the readout neurons for the activity of the CA3 place cells. Assuming that contemporaneous spiking of place cells implies overlap of their respective place fields (Figure 1A-B), it is possible to decode the rat’s current location from the ongoing spiking activity of a mere 40-50 neurons [21]. This suggests that the readout neurons may be wired to encode spatial connectivity between place fields by responding to place cell coactivity (see Figure 1A-C and [22–24]).

A natural assumption underlying both the trajectory reconstructing algorithms [21] and various path integration models [3, 27, 29] is that the representation of spatial locations during physical navigation is reproducible. If the rat begins locomotion at a certain location and at a certain moment of time, t_0 , and then returns to the same location at a later time, t_1 , then the population activity of the place cells at t_0 and t_1 is the same. Similarly, if spatial information is consistently represented during replays, then the activity packet in the hippocampal network should be restored upon “replaying” a closed path. Whereas the correspondence between place cell activity and spatial locations (i.e., place fields) during physical navigation is enforced by sensory and proprioceptive inputs [27], the consistency of spatial representation during replay must be attributable solely to the network’s internal dynamics [28].

Here we develop a model that accounts for how a neuronal network could maintain consistency of spatial information over the course of multiple replays or preplays. This model is based on the discrete differential geometry theory developed in [30], which reveals that key geometric concepts can be expressed in purely combinatoric terms. The choice of this theory is driven in part by recent work that indicates that the hippocampus provides a topological framework for spatial information rather than a geometric or Cartesian map [24–26].

The results suggest that to maintain consistency of spatial information during path replay, the synaptic connections between the place cells and the readout neurons must adhere to a zero holonomy principle.

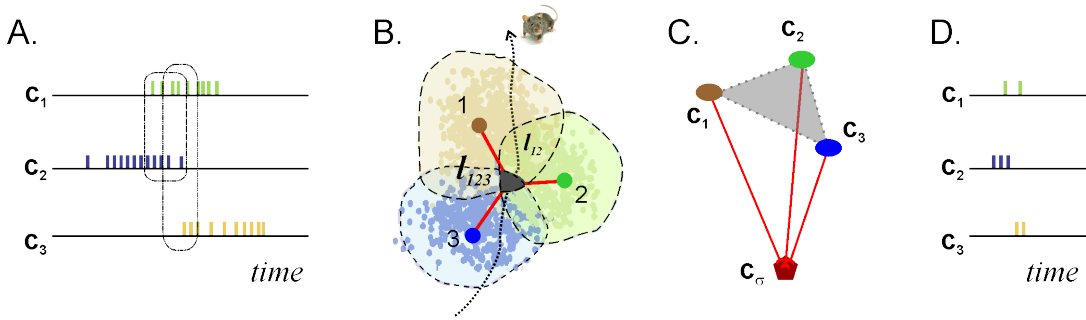


FIG. 1: Place cells, place fields and cell assemblies. **A.** A schematic representation of the spike trains produced by three place cells, c_1 , c_2 and c_3 . The two red rectangles mark the periods during which the cells are coactive [38]. **B.** The gold, green and blue areas represent place fields. Place cell firing rate is maximal at the center of the place field and attenuates towards its periphery; this pattern can be closely approximated by Gaussian distribution. Place cell cofiring reflects overlap between respective place fields: cells c_1 and c_2 are coactive in the location l_{12} , cells c_2 and c_3 are coactive in the location l_{23} and so on. The red links mark distances between the centers of the place fields and the triple overlap domain, l_{123} (dark region in the center). **C.** A schematic representation of a cell assembly: the three place cells on the top synapse onto a readout neuron (red dot), which activates within the cell assembly field l_{123} . **D.** During replay, the place cells repeat on a millisecond time scale the order of spiking that they exhibit during active navigation.

II. THE MODEL

The simplicial model of the cell assembly network. A convenient framework for representing a population of place cell assemblies is provided by simplicial topology [32–34]. In this approach, an assembly of $d + 1$ place cells, $\{c_{i_0}, c_{i_1}, \dots, c_{i_d}\}$, is represented by a d -dimensional abstract simplex (not to be confused with a geometric simplex) containing $d + 1$ vertexes, $\sigma = [v_{i_0}, v_{i_1}, \dots, v_{i_d}]$, where each vertex, v_i , corresponds to a place cell c_i (in the following, the same symbol “ σ ” will be used to denote a cell assembly and the simplex that represents it) [37, 38]. The entire network can then be represented by a purely combinatorial simplicial complex \mathcal{T} [31, 32] whose *maximal* simplexes correspond to place cell assemblies [39]. Simplexes in \mathcal{T} may overlap: physiological studies demonstrate that a given place cell may be a part of many cell assemblies [40, 41]. Many authors have suggested that place cell assemblies should overlap significantly in order to better represent contiguous spatial locations [46–49]: the more cells shared by σ_1 and σ_2 , the closer the encoded locations are to one another. The most detailed representation of the environment is produced by a population of maximally overlapping cell assemblies, which differ by a single cell. In such case, a transition of the activity from one cell assembly σ_1 to another σ_2 occurs when one place cell in σ_1 turns off and another cell in the new assembly σ_2 turns on. The resulting simplicial complex \mathcal{T} has the structure of a combinatorial d -dimensional simplicial manifold (in the literature also referred to as “pure complex” or “pseudomanifold”, [31]).

Population activity in the cell assembly complex \mathcal{T} . The simplicial complex \mathcal{T} is a convenient instrument for relating place cell coactivity to the topology of the rat’s environment [37, 38]. The rat’s movements in the physical environment induce a packet of place cell activity that propagates in the hippocampal network—an “activity bump” [27]. In our model the propagation of the activity bump corresponds to an “active simplex” propagating through \mathcal{T} . The resulting population activity vector is then

$$\mathbf{f}_\sigma^\top = (f_\sigma, f_{\sigma, v_{i_0}}, f_{\sigma, v_{i_1}}, \dots, f_{\sigma, v_{i_k}}), \quad (1)$$

where the first component f_σ represents the spiking rate of the readout neuron, and f_{σ, v_i} denotes the spiking rate of the place cell c_i within the assembly σ . Roughly speaking, f_{σ, v_i} can be viewed as the firing rate of

c_i at the location where the place fields of the cells constituting the assembly σ overlap, which we refer to as the cell assembly field, l_σ (the domain l_{123} on Figure 1B). A given place cell c_i is a part of many cell assemblies $\sigma_1, \sigma_2, \dots$, whose fields $l_{\sigma_1}, l_{\sigma_2}, \dots$ are contained in the c_i 's place field; thus, the higher the orders of the cell assemblies, the (statistically) smaller the l_σ s [39]. Since the individual place cell spiking rates are well approximated by smooth Gaussian functions of the rat's coordinates [36], the quantities f_{σ, v_i} remain approximately constant over l_σ . The components of the population activity vector (1) in a given cell assembly can then be related to the corresponding place cells' maximal firing rates f_{v_i} by a set of factors $0 \leq h_{\sigma, v_i} \leq 1$, that are specific to a given cell and a given cell assembly,

$$f_{\sigma, v_i} = h_{\sigma, v_i} f_{v_i}, \quad (2)$$

which may be viewed as measures of the separation between the location l_σ and the respective place fields' centers (Figure 1B). In other words, the coefficients h_{σ, v_i} provide a discrete description of the place field map's geometry.

As the rat moves from one cell assembly field to another (e.g., from l_{σ_1} to l_{σ_2}), the activity packet in \mathcal{T} shifts from the maximal simplex σ_1 to the maximal simplex σ_2 , then to σ_3 , and so on, tracing a ‘‘simplicial path,’’

$$\Gamma = \langle \sigma_1, \sigma_2, \dots, \sigma_n \rangle, \quad (3)$$

(these are ‘‘thick paths’’ in the terminology of [30]). As a result, every path γ in the rat's physical environment corresponds to a simplicial path $\Gamma \in \mathcal{T}$, which can be viewed as an abstract representation of the place cell trajectory code used in [21]. However, in order to represent the path Γ in the hippocampal network, the activity of each place cell assembly $\sigma \in \Gamma$ should activate the corresponding readout neuron c_σ . Thus, during the activation period, the net input from the presynaptic cells in σ should exceed the corresponding readout neuron's firing threshold θ_σ ,

$$\sum_{v_i \in \sigma} w_{\sigma, v_i} f_{\sigma, v_i} \geq \theta_\sigma, \quad (4)$$

where the coefficients w_{σ, v_i} represent the strengths of synaptic connections between the place cells and the readout neuron [20, 61].

In other words, this is a rate model in that the activity of cells is described by a single parameter: the firing rate, f , related via coefficients h to the maximal rate (2). If the network is trained—the synaptic architecture is fixed, place fields are stable—then each cell assembly fires when the rat visits (or replays) a specific spot where the respective place fields overlap. Because this spot is very small compared to the size of place fields, the left side of (4) is essentially the same every time.

Using (2), the condition (4) becomes

$$\sum_{v_i \in \sigma} b_{\sigma, v_i} f_{v_i} \geq \theta_\sigma, \quad (5)$$

where the variables θ and

$$b_{\sigma, v_i} = w_{\sigma, v_i} h_{\sigma, v_i}, \quad (6)$$

are defined on all simplexes (i.e., all cell assemblies), and the variable f on the vertexes (i.e., place cell).

Dressed cell assembly complex \mathcal{T}_* . The coefficients b_{σ, v_i} can be regarded as characteristics of the maximal simplexes of \mathcal{T} and the values f_{v_i} as characteristics of its vertexes. Together, these parameters produce a ‘‘dressing’’ of the cell assembly complex with physiological information about the cells' spiking and the network's synaptic architecture. Equation (5) singles out a set $\mathcal{B}_{\mathcal{T}_*}$ of *valid dressings*, $\mathcal{B}_{\mathcal{T}_*} = \{b_{\sigma, v} : \text{eq. (5) is satisfied}\}$ which enable readout neurons to respond to presynaptic activity and thus defines the scope of working synaptic architectures of the place cell assembly networks.

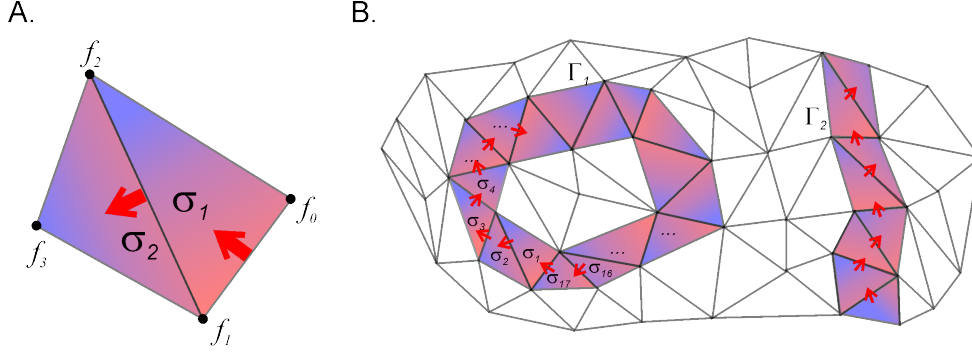


FIG. 2: **Propagation of place cell activity along simplicial paths.** **A.** The firing rate of the cell c_2 , required to activate the readout neuron of the cell assembly σ_1 , can be inferred from the firing rates of the other two cells, c_0 and c_1 using the equation (10) (red arrow over σ_1). The the resulting rate f_2 of c_2 and the rate f_0 of c_0 define the rate f_3 of the cell c_3 required to activate the readout neuron in the next cell assembly σ_2 according to the equation (11) (red arrow over the σ_2). **B.** A network of maximally overlapping cell assemblies is represented by a simplicial manifold \mathcal{T}_* . The replayed sequences correspond to simplicial paths that can be closed (Γ_1) or open (Γ_2).

Replays occur on a millisecond time scale and produce only a few spikes per activity period [19] (Figure 1D), which is comparable to the stochastic background activity of neurons. In order to distinguish cell assembly activation from the assembly's background activity, the readout neuron should be tuned to a particular combination of inputs; the physiological process most likely involves gating specific parts of the dendritic tree by timed inputs from the presynaptic cells. Here, the model employs a simplified version of this process: we propose that the readout neuron should remain in a sensitive, near-threshold state [50] that allows it to quickly respond to the cell assembly during each individual step of replay. Thus, we hypothesize that during replays the inequality (5) may be approximated by the equation

$$\sum_{v_i \in \sigma} b_{\sigma, v_i} f_{v_i} = \theta_{\sigma}, \quad (7)$$

which further restricts the set of valid dressings to a special marginal set $\bar{\mathcal{B}}_{\mathcal{T}_*}$, for which spontaneous replays of place cell assemblies are possible. Note, however, that equation (7) does not fix the values of the parameters f_{v_i} and b_{σ, v_i} , and so it allows a significant variability of spiking activity and of the synaptic connection strengths. To emphasize the assumption that place cell activity during replays elicits a response from the readout neuron at a constant rate $f_{\sigma} > 0$, it is convenient to use the notation

$$\theta_{\sigma} \equiv b_{\sigma, \sigma} f_{\sigma}, \quad (8)$$

where $b_{\sigma, \sigma} > 0$ is a fixed parameter that can be interpreted as the readout neuron's susceptibility to discharge.

Replays. Equation (7) defined at each simplex of \mathcal{T}_* [30] provides a simple tool for building a model of hippocampal replay. As an illustration, consider the case when \mathcal{T}_* is two-dimensional and let $\sigma_1 = [v_0, v_1, v_2]$ be a 2D simplex representing an assembly of three cells with the firing rates f_{v_0} , f_{v_1} and f_{v_2} . If equation (7) holds over σ_1 , then the readout neuron c_{σ_1} fires with the rate f_{σ_1} in response to the coactivity of c_1 , c_2 and c_3 ,

$$b_{\sigma_1, v_0} f_{v_0} + b_{\sigma_1, v_1} f_{v_1} + b_{\sigma_1, v_2} f_{v_2} = b_{\sigma_1, \sigma_1} f_{\sigma_1}. \quad (9)$$

Suppose that equation (7) also holds for an adjacent (maximally overlapping) cell assembly, represented by an adjacent simplex $\sigma_2 = [v_1, v_2, v_3]$, so that the second readout neuron c_{σ_2} fires with the rate f_{σ_2}

$$b_{\sigma_2, v_1} f_{v_1} + b_{\sigma_2, v_2} f_{v_2} + b_{\sigma_2, v_3} f_{v_3} = b_{\sigma_2, \sigma_2} f_{\sigma_2}. \quad (10)$$

A key observation here is that, since σ_2 shares vertexes v_1 and v_2 with σ_1 , the corresponding firing rates f_{v_1} and f_{v_2} in (10) define uniquely the firing rate of the remaining cell, f_{v_3} , required to activate the readout neuron c_{σ_2} (Fig. 2A),

$$f_{v_3} = \frac{1}{b_{\sigma_2, v_3}}(b_{\sigma_2, \sigma_2} f_{\sigma_2} - b_{\sigma_2, v_1} f_{v_1} - b_{\sigma_2, v_2} f_{v_2}). \quad (11)$$

Similarly, if there is another $2D$ simplex $\sigma_3 = [v_2, v_3, v_4]$ adjacent to σ_2 , then, once the value f_{v_3} is found from (11), the firing rate at v_4 can be obtained from f_{v_2} and f_{v_3} , and so on (Figure 2B). In other words, once the synaptic connections $b_{\sigma, v}$ are specified for all simplexes, equation (7) can be used to describe the conditions for transferring the activity vector \mathbf{f}_σ over the entire complex \mathcal{T}_* [30]. Notice however, that equations (9)-(11) do not specify the mechanism responsible for generating place cell activity; they only describe the conditions required to ignite the cell assemblies in a particular sequence. While the subsequent simplexes σ_n and σ_{n+1} in the simplicial path (3) are not necessarily adjacent, the activity according to equation (7) is propagated along a sequence of adjacent maximal simplexes, such as depicted in Figure 2B.

Discrete Holonomy. Using the notation

$$\mu_{x,y}^\sigma \equiv \frac{b_{\sigma,x}}{b_{\sigma,y}}, \quad (12)$$

equation (11) defined over a simplex σ_p can be rewritten in matrix form

$$\mathbf{f}_q = M_{q,p}^{v_i v_s} \mathbf{f}_p, \quad (13)$$

where the ‘‘transfer matrix’’ $M_{q,p}^{v_i v_s}$ propagates the population activity vector from the incoming facet of the simplex σ_p into the activity vector of the outgoing, opposite facet shared with the next simplex σ_q (edges $[v_0, v_1]$ and $[v_1, v_2]$ respectively on Figure 2A), in which the vertex v_s of the simplex σ_p shuts off and the vertex v_t of the adjacent simplex activates. If there is a total of n simplexes in the path Γ ($n = 17$ for the closed simplicial path Γ_1 shown on Figure 2B) then the corresponding chain of n equations (13) will produce

$$\mathbf{f}_n = M_{q_n, p_n}^{v_i v_s} M_{q_{n-1}, p_{n-1}}^{v_i v_s} \dots M_{q_1, p_1}^{v_i v_s} \mathbf{f}_1. \quad (14)$$

If the simplicial path is closed, then the activity vector should be restored upon completing the loop, i.e., $\mathbf{f}_n = \mathbf{f}_1$. According to (14), this will happen if the product of the transfer matrices along Γ yields a unit matrix,

$$M_\Gamma \equiv M_{q_n, p_n}^{v_i v_s} M_{q_{n-1}, p_{n-1}}^{v_i v_s} \dots M_{q_1, p_1}^{v_i v_s} = \mathbf{1}. \quad (15)$$

It can be directly verified, however, that condition (15) is not satisfied automatically: the product of transfer matrices (15) has the structure

$$M_\Gamma = \begin{pmatrix} 1 & 0 & 0 \\ 0 & 1 & 0 \\ \kappa_{\Gamma,1} & \kappa_{\Gamma,2} & 1 + \kappa_{\Gamma,3} \end{pmatrix}, \quad (16)$$

which differs from the unit matrix $M_\Gamma \neq \mathbf{1}$ (see Appendix). This implies that a population activity vector \mathbf{f}_σ is in general altered by translations around closed simplicial paths, $\mathbf{f}_\sigma(t_{\text{start}}) \neq \mathbf{f}_\sigma(t_{\text{end}})$. To formulate this another way, the spiking condition (7) does not automatically guarantee that the readout neurons will consistently represent spatial connectivity; the latter requires additional constraints (15), irrespective of the mechanism that shifts the activity bump.

Mathematically, a mismatch between the starting and the ending orientation of the population activity vector is akin to the differential-geometric notion of holonomy which, on Riemannian manifolds, measures

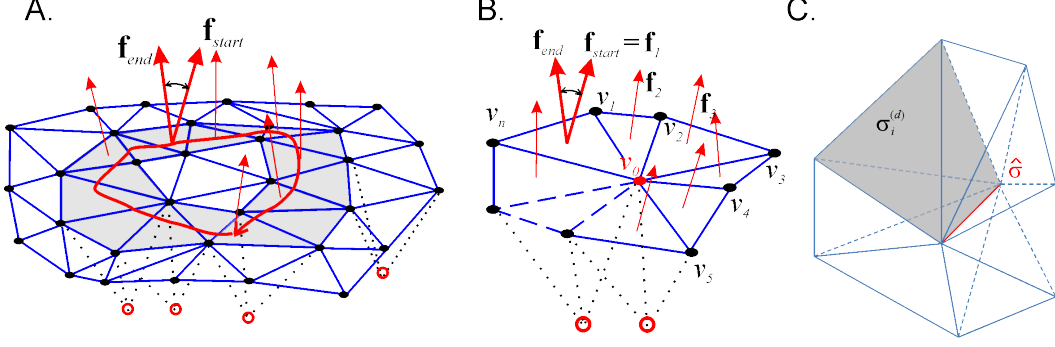


FIG. 3: **Discrete geometry of a dressed simplicial complex.** **A.** Discrete holonomy: a population activity vector (red arrow) changes its direction from simplex to simplex as described by (13). Upon completing a closed path, the starting and ending vectors may differ, $\mathbf{f}_{start} \neq \mathbf{f}_{end}$, which indicates nonzero holonomy. **B.** A 2D elementary closed path of the order n encircling a vertex v_0 . The “pivot” vertex v_0 carries the discrete curvature coefficients defined by (17). **C.** A higher dimensional elementary closed path consisting of d -dimensional simplexes (one such exemplary simplex $\sigma_1^{(d)}$ is shadowed) sharing the same $(d - 2)$ -dimensional face, the pivot simplex $\hat{\sigma}_1$, shown in red. The $d - 2$ dimensional pivot simplex $\hat{\sigma}$ shown in red carries the curvature coefficients $\kappa_{\hat{\sigma},i}$.

the change of a vector’s orientation as a result of a parallel transport around a closed loop [30, 33–35]. Hence, the requirement (15) that the activity vector should be the same after completing a closed simplicial trajectory implies that the discrete holonomy along paths in \mathcal{T}_* should vanish.

Discrete Curvature. In differential geometry, zero holonomy on a Riemannian manifold is achieved by requiring that the Riemannian curvature tensor R^i_{jkl} associated with the connection Γ^i_{jk} vanishes at every point x [34, 35]. This condition is established by contracting closed paths to infinitesimally small loops encircling a point x and translating in parallel a unit vector \vec{n} around that loop. The difference between the starting and the ending orientations of \vec{n} defines the curvature at the point x [35]. An analogous procedure can be performed on a discrete manifold \mathcal{T}_* . However, there is a natural limit to shrinking simplicial paths: in a d -dimensional complex, the tightest simplicial paths consist of d -dimensional simplexes $\sigma^{(d)}$ which intersect the same $(d - 2)$ dimensional face (see Figure 3B). Such a path $\Gamma_{\sigma^{(d-2)}}$ we will call an “elementary closed path”, following [30]. The order s_n of such a path is defined by the number of d -dimensional simplexes $\sigma^{(d)}$ encircling a simplex $\sigma^{(d-2)}$. In the following we will use the short notation $\hat{\sigma}$ for the “pivot” simplexes $\hat{\sigma} \equiv \sigma^{(d-2)}$ whereas the elementary simplicial path encircling $\hat{\sigma}$ will be denoted as $\Gamma_{\hat{\sigma}}$.

In order to ensure zero holonomy of place cell activity along *all* closed paths in \mathcal{T}_* , it is sufficient to verify that the holonomy vanishes for all elementary closed paths [30]. The product of the matrices $M_{q,p}^{v_i v_s}$ encircling the pivot $\hat{\sigma}$ (Figure 3B) has the same form as equation (16); however, the coefficients $\kappa_{\hat{\sigma},i}$ at the bottom row of the matrix $M_{\hat{\sigma}}$ can be viewed as the curvatures defined at $\hat{\sigma}$. Thus, to ensure zero holonomies, the conditions

$$\kappa_{\hat{\sigma},i} = 0, \quad (17)$$

$i = 1, \dots, d + 1$, must be imposed on the connection coefficients b_{σ,v_i} at every pivot simplex $\hat{\sigma}$ of a d -dimensional dressed cell assembly simplicial complex. For example, an elementary 2D closed path encircling a vertex v_0 with n simplexes enumerated as shown on Figure 3C yields the holonomy matrix

$$M_{v_0} = \begin{pmatrix} 1 & 0 & 0 \\ 0 & 1 & 0 \\ \kappa_{v_0,1} & \kappa_{v_0,2} & 1 + \kappa_{v_0,3} \end{pmatrix}.$$

The values $\kappa_{v_0,i}$, $i = 1, 2, 3$, of the bottom row that distinguish M_{v_0} from the unit matrix should be considered as discrete curvatures defined at the pivot vertex v_0 (see Figure 3C and [30]), which need to vanish in order to ensure a consistent representation of space during replays.

Since there exists a finite number of pivot simplexes, the number of constraints (17) on a given dressing $b_{\mathcal{T}} \in \bar{\mathcal{B}}_{\mathcal{T}_*}$ is finite. Thus, the scope of nontrivial zero holonomy conditions (15) drastically reduces and the task of ensuring consistency of translations of the population activity vectors over \mathcal{T}_* becomes tractable. Nevertheless, zero curvature conditions (17) are in general quite restrictive and impose nontrivial constraints on the synaptic architecture of the place cell assemblies. As the simplest illustration, consider the case when the firing rates of all the place cells and readout neurons are the same: $f_{v_i} = f_{\sigma_k} = f$, and all the connection strengths from the place cells to the readout neuron in all cell assemblies are identical: $b_{\sigma_i, v_i} = \bar{b}$, giving a constant connection dressing $\bar{b}_{\mathcal{T}_*}$. It can be shown that in this case the resulting transfer matrix is idempotent, that is $M_{\bar{\sigma}}^2 = \mathbf{1}$, so that the zero curvature condition (17) is satisfied identically for the even order elementary closed paths and cannot be satisfied if the paths' order is odd. Under more general and physiologically more plausible assumptions equation (17) does not necessarily restrict the order of the cell assemblies. However, the domain of permissible dressings, $\bar{\mathcal{B}}_{\mathcal{T}_*}$ is significantly restricted by (17), as compared to the domain occupied by the synaptic parameters of the unconstrained cell assembly networks.

III. STATISTICS OF SYNAPTIC WEIGHTS IN THE LIMIT OF WEAK SYNAPTIC NOISE

The zero curvature constraints (17) affect the net statistics of the synaptic weights. Since the structure of the full space of marginal dressings $\bar{\mathcal{B}}_{\mathcal{T}_*}$ and of the corresponding probability measures is too complex, we considered a family of connections parametrized as

$$b_{\sigma, v} = \bar{b} \left(1 + \varepsilon_{\sigma, v} + O(\varepsilon_{\sigma, v}^2) \right), \quad (18)$$

in which the fluctuations $\varepsilon_{\sigma, v}$ are normally distributed,

$$P(\varepsilon_{\sigma, v}) = \frac{1}{\varepsilon \sqrt{\pi}} e^{-\frac{\varepsilon_{\sigma, v}^2}{\varepsilon^2}}. \quad (19)$$

In the absence of zero curvature constraints, cell assemblies are uncoupled and the synaptic fluctuations are statistically independent, so that the joint probability distribution of $\varepsilon_{\sigma, v}$ is

$$\mathcal{P}(\varepsilon) = \prod_{\sigma, v} P(\varepsilon_{\sigma, v}). \quad (20)$$

Under zero-curvature conditions (17) the parameters of the synaptic architecture are coupled (Figure 5) and the probability distribution for a particular variable $\varepsilon_{\sigma, v}$ is obtained by averaging the joint distribution (20) under delta-constraints:

$$\hat{P}(\varepsilon_{\sigma, v}) = C \int \cdots \int \prod_{\hat{\sigma}} \prod_{i=1}^{d+1} \delta(\kappa_{\hat{\sigma}, i}(\varepsilon)) \mathcal{P}(\varepsilon) D' \varepsilon, \quad (21)$$

where C is the normalization constant and $D' \varepsilon \equiv \prod' d\varepsilon_{\sigma, v}$ denotes integration over all $\varepsilon_{\sigma', v'} \neq \varepsilon_{\sigma, v}$.

In the Appendix it is demonstrated that for weak fluctuations, the shape of the distribution (19) remains Gaussian,

$$\hat{P}(\varepsilon_{\sigma, v}) = \frac{1}{\sqrt{\pi \varepsilon_*}} e^{-\frac{\varepsilon_{\sigma, v}^2}{\varepsilon_*^2}} \quad (22)$$

but its width decreases: $\varepsilon_* < \varepsilon$. Thus, zero curvature conditions narrow the distribution of the uncorrelated weights, i.e., produce a ‘‘tuning’’ of the synaptic connections $b_{\sigma, v}$. This result also applies to the synaptic weights: in cases where the place fields are distributed regularly, so that the coefficients h_{σ, v_i} have a well defined mean, \bar{h} , and a small multiplicative variance,

$$h_{\sigma, v_i} = \bar{h} (1 + \delta_{\sigma, v_i}),$$

$\delta_{\sigma,v_i} \ll 1$, the coefficients μ_{v_1,v_2}^σ are approximately defined by the ratios of the synaptic weights,

$$\mu_{v_1,v_2}^\sigma = \frac{b_{\sigma,v_1}}{b_{\sigma,v_2}} = \frac{w_{\sigma,v_1} h_{\sigma,v_1}}{w_{\sigma,v_2} h_{\sigma,v_2}} = \frac{w_{\sigma,v_1}}{w_{\sigma,v_2}} (1 + \delta_{\sigma,v_1} - \delta_{\sigma,v_2}) \approx \frac{w_{\sigma,v_1}}{w_{\sigma,v_2}},$$

and therefore the zero curvature conditions produce the same effect on $w_{\sigma,v}$ as on $b_{\sigma,v}$, i.e., reduce the variability of synaptic weights.

Understanding the effects produced by zero curvature constraints (17) on a wider range of fluctuations is mathematically more challenging. The qualitative results obtained here, however, may generalize beyond the limit of small multiplicative synaptic noise and could eventually be experimentally verified. A physiological implication of the result (22) is that the distribution of the unconstrained synaptic weights in a network that does not encode a representation of space (e.g., measured *in vitro*) should be broader than the distribution measured *in vivo* in healthy animals, which can be tested once such measurements become technically possible.

IV. DISCUSSION

The task of encoding a consistent map of the environment imposes a system of constraints on the hippocampal network (i.e., on the coefficients $b_{\sigma,v}$) that enforce the correspondence between place cell activity and the animal’s location in the physical world. Here we show that zero holonomy is a key condition, which is implemented by requiring that curvatures vanish at the pivot simplexes. This approach works within a combinatorial framework, but a similar intuition guided a geometric approach [29], where the place cells’ ability to encode the location of the animal—but not the path leading to that location—was achieved by imposing the conditions of Stoke’s theorem [34] on the synaptic weights of the hippocampal network, which were viewed as functions of Cartesian coordinates. Our model is based on the same requirement of path-invariance of place cell population activity, implemented on a discrete representation of space—a dressed abstract simplicial complex \mathcal{T}_* —without involving geometric information about the animal’s environment.

In particular, note that the concepts of “curvature” and “holonomy” are defined in combinatorial, not geometric, terms. This is an advantage in light of (and indeed was motivated by) recent work indicating that the hippocampus provides a topological framework for spatial experience rather than Cartesian map of the environment [24], and it also makes our model somewhat more realistic. It does, however, lead to a number of technical complications. For example, discrete connections (6) defined over \mathcal{T}_* are nonabelian [30], so using the approach of [29] would require a nontrivial generalization of Stoke’s theorem, which is valid only in spaces with abelian differential-geometric connections [51]. Our approach is based on the analysis of discrete holonomies suggested in the pioneering work of [30] which, in fact, explains the mathematical underpinning of the Stoke’s theorem approach in both abelian and nonabelian cases [33–35]. Indeed, the zero-holonomy constraint ensures that no matter what direction the activity is propagated in the network (forward, backward, or skipping over some cell assemblies), the integrity of the spatial information remains intact.

Generality of the approach. A key instrument of our analyses is equation (7), which describes the conditions necessary for propagating spiking conditions over the cell assembly network. The exact form of this equation is not essential—a physiologically more detailed description of near-threshold neuronal spiking [52–54] could be used to establish more accurate zero holonomy and curvature constraints on the hippocampal network’s synaptic architecture, which should be viewed as a general requirement for any spatial replay model.

The assumption of maximally-overlapping place cell assemblies may also be relaxed, since equation (7) can be applied in cases where the order of the cell assemblies varies, that is, when the simplicial complex \mathcal{T}_* is not a manifold but a quasimanifold (see Figure 4 and [55, 56]). Unfortunately, implementing the “zero holonomy” principle in this case would require rather arduous combinatorial analysis. For example,

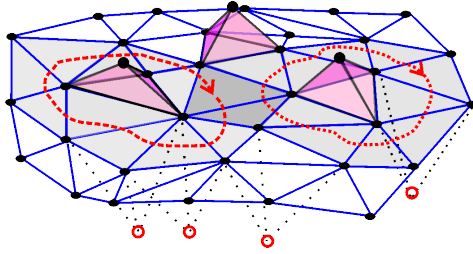


FIG. 4: **A replay in simplicial quasimanifold.** An example of a simplicial quasi-manifold containing $2D$ and $3D$ simplices. The activity of cells in the $3D$ simplices is induced from the $2D$ simplices approaching its sides. Two simplicial paths are shown by gray triangles, marked by red dotted lines.

propagating the activity packets using (14) would impose relationships between the dimensionalities of the maximal simplices and their placement in \mathcal{T}_* , i.e., require a particular cell assembly network architecture.

Learning the constraints. In this paper, the requirements (15) and (17) enforcing path consistency of place cell replay are imposed on a fully trained network: it is assumed that the place fields have had time to stabilize [59] and that the cell assemblies with constant weights w_{σ, v_i} have had time to form [4]. In a more realistic approach, these constraints should modulate the hippocampal network’s training process. For example, if the unconstrained network is trained by minimizing a certain cost functional $S(b_{\mathcal{T}_*})$ [18, 62] then the constraints (17) would contribute an additional “curvature term” $R(b_{\mathcal{T}_*})$,

$$S(b_{\mathcal{T}_*}) \rightarrow S(b_{\mathcal{T}_*}) + R(b_{\mathcal{T}_*}), \quad (23)$$

defined, e.g., via Lagrange multipliers r_i ,

$$R(b_{\mathcal{T}_*}) = \sum_{\hat{\sigma} \in \mathcal{T}_*} R_{\hat{\sigma}}(b_{\mathcal{T}_*}) = \sum_{\hat{\sigma}, i} r_i \kappa_{\hat{\sigma}, i}. \quad (24)$$

Physiologically, the network may be trained by “ringing out” the violations of the conditions (17) in the neuronal circuit, i.e., by replaying sequences and adapting the synaptic weights to get rid of the centers of non-vanishing holonomy. Curiously, the role played by $R(b_{\mathcal{T}_*})$ in (23) resembles the role played by the curvature term in the Hilbert–Einstein action of General Relativity Theory [34], which ensures that, in the absence of gravitational field sources, the solution of the Hilbert–Einstein equations describes a flat space-time. By analogy, the constraints imposed by (17) may be viewed as conditions that enforce “synaptic flatness” of the hippocampal cognitive map.

It is worth noting that the mechanism suggested here is an implementation of the zero holonomy condition in this simplest case of the reader-centric cell assembly theory that is consistent with physiology. The place cell readout might involve, instead of a single neuron, a small network of a few neurons (not yet identified experimentally), which might require a different implementation of zero holonomy principle, depending on the specific architecture of such a network. If the readout network is a cluster of synchronously activated downstream neurons, then this cluster of cells could be viewed as a “meta-neuron” and the proposed approach would apply to this case as well. More complicated architectures would require modifications, but it is reasonable that the reproducibility of the population vector would require zero holonomy in all cases.

V. ACKNOWLEDGMENTS

I thank V. Brandt and R. Phenix for their critical reading of the manuscript and the reviewers for helpful comments..

The work was supported in part by Houston Bioinformatics Endowment Fund, the W. M. Keck Foundation grant for pioneering research and by the NSF 1422438 grant.

VI. APPENDIX

Transfer matrix construction is carried out for the $2D$ case, since higher dimensions are similar. In the matrix form, equation (11) defined over the simplex σ_p , can be written as $\mathbf{f}_q = \hat{M}_{q,p}^{v_k v_j} \mathbf{f}_p$, in which the matrix

$$\hat{M}_{q,p}^{v_k v_j} = \begin{pmatrix} 1 & 0 & 0 \\ 0 & 1 & 0 \\ \mu_{\sigma_p, v_k}^{\sigma_p} & -\mu_{v_i, v_k}^{\sigma_p} & -\mu_{v_j, v_k}^{\sigma_p} \end{pmatrix},$$

transfers the activity vector

$$\mathbf{f}_p^\top = (f_{\sigma_p}, f_{v_i}, f_{v_j}),$$

defined over the incoming edge $[v_i, v_j]$ of the p -th simplex into the activity vector at the outgoing edge $[v_i, v_k]$ of the *same* simplex (e.g., from the edge $[v_0, v_1]$ to the edge $[v_1, v_2]$ of σ_1 on Figure 2A),

$$\mathbf{f}_p^\top = (f_{\sigma_p}, f_{v_i}, f_{v_k}). \quad (25)$$

To ignite the readout neuron of the next cell assembly σ_q , which shares the edge $[v_i, v_k]$ with σ_p the vector (25) needs to be transformed into

$$\mathbf{f}_q^\top = (f_{\sigma_q}, f_{v_i}, f_{v_k})$$

by the diagonal matrix $D_{p,q} = \text{diag}(f_{\sigma_q}/f_{\sigma_p}, 1, 1)$. Together, these two operations produce the transfer matrix

$$M_{q,p}^{v_k v_j} = D_{p,q} \hat{M}_{q,p}^{v_k v_j} = \begin{pmatrix} f_{\sigma_q}/f_{\sigma_p} & 0 & 0 \\ 0 & 1 & 0 \\ \mu_{\sigma_p, v_k}^{\sigma_p} & -\mu_{v_i, v_k}^{\sigma_p} & -\mu_{v_j, v_k}^{\sigma_p} \end{pmatrix}.$$

A direct verification shows that a product of n transfer matrices that start and end at the same simplex, has the form (16), in which $\kappa_{\Gamma, i}$ are n th order polynomials of the coefficients (12).

Tuning of the fluctuation distribution. In case when the fluctuations are small, $\varepsilon \ll 1$, the constraints (17) uncouple (Figure 5) yielding linearized curvature coefficients

$$\kappa_{\hat{\sigma}, i} = \sum_{v \in \Gamma_{\hat{\sigma}}} Q_{\hat{\sigma}, i; \sigma, v} \varepsilon_{\sigma, v}, \quad (26)$$

where $Q_{\hat{\sigma}, i; \sigma, v}$ are constant coefficients and the summation is over the vertexes of the elementary path $\Gamma_{\hat{\sigma}}$ (Figure 3B). To simplify the expression (21), we rewrite it using indexes $p = (\sigma, v)$ and $l = (\hat{\sigma}, i)$,

$$\hat{P}(\varepsilon_p) = C \int \cdots \int \prod_l \delta(\kappa_l(\varepsilon_{p'})) \mathcal{P}(\varepsilon_{p'}) \prod_{p' \neq p} d\varepsilon_{p'},$$

and exponentiate the delta-functions,

$$\hat{P}(\varepsilon_p) = C \int \cdots \int \int_{\eta=-\infty}^{\infty} \cdots \int \mathcal{P}(\varepsilon_{p'}) \prod_l d\eta_l e^{i\eta_l \kappa_l} \prod_{p' \neq p} d\varepsilon_{p'}. \quad (27)$$

Using the joint distribution (20) and the linearized expressions (26) in (27) produces

$$\hat{P}(\varepsilon_p) = C e^{-\frac{\varepsilon_p^2}{\varepsilon^2}} \int_{\eta=-\infty}^{\infty} \cdots \int \prod_l d\eta_l e^{i\eta_l V_{lp} \varepsilon_p} \int \cdots \int \prod_{p' \neq p} d\varepsilon_{p'} e^{-\frac{\varepsilon_{p'}^2}{\varepsilon^2}} e^{i\eta_l V_{lp'} \varepsilon_{p'}},$$

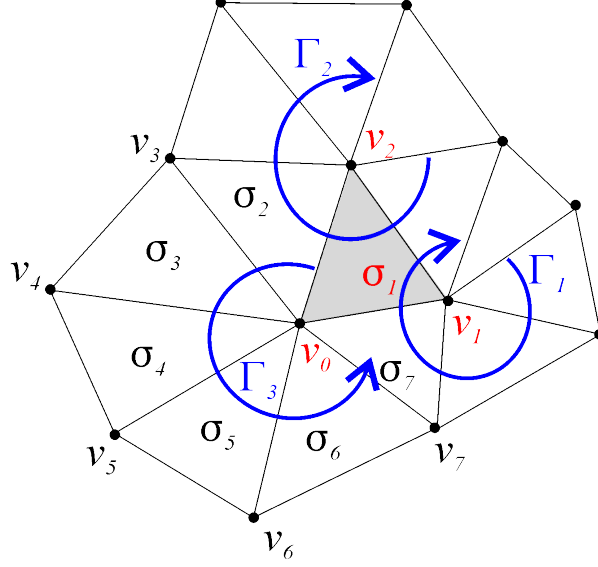


FIG. 5: **Coupling between simplices.** A schematic illustration of a maximal simplex σ_1 span by three pivot vertexes, v_0 , v_1 and v_2 , and shared by three overlapping elementary paths Γ_1 , Γ_2 and Γ_3 in a 2D cell assembly complex. As a result, the synaptic connectivity coefficients $b_{\sigma_1, v}$ will appear in three sets of discrete curvatures, $\kappa_{v_0, i}$, $\kappa_{v_1, i}$ and $\kappa_{v_2, i}$, $i = 1, 2, 3$, bootstrapping the constraints (17).

where the V_{lp} are the coefficients obtained by collecting the terms proportional to ε_p 's produced by (26). Completing the square and integrating over ε_p yields a Gaussian integral over a positive quadratic form $A = VV^T$,

$$\hat{P}(\varepsilon_p) = e^{-\frac{\varepsilon_p^2}{\varepsilon^2}} \int \dots \int_{\eta=-\infty}^{\infty} \prod_l d\eta_l e^{i\varepsilon_p v_p \eta} e^{-\frac{1}{4}\varepsilon^2(\eta A \eta)}. \quad (28)$$

where v_p is the p th row of the matrix V . Evaluating (28) yields

$$\hat{P}(\varepsilon_p) = C e^{-\frac{\varepsilon_p^2}{\varepsilon^2} - \frac{\varepsilon_p^2}{\varepsilon^2} v_p A^{-1} v_p} = C e^{-\frac{\varepsilon_p^2}{\varepsilon_*^2}} \quad (29)$$

where

$$\varepsilon_*^2 = \varepsilon^2 \left(1 + v_p A^{-1} v_p\right)^{-1}. \quad (30)$$

Since the second term in the parentheses is positive, $\varepsilon_* < \varepsilon$, which indicates narrowing of the uncoupled distribution (19). The magnitude of the correction in (30) depends on the topological structure of the coactivity complex (e.g., its dimensionality d and the statistics of the pivots' orders, n) and on the dressing parameters, $\bar{\mathcal{B}}_{\mathcal{T}_*}$. In the approximation (18), $\varepsilon \ll 1$, the diagonal matrix elements of the matrix A are of the order $d\bar{n}$, and hence the $v_p A^{-1} v_p \sim d/\bar{n}$.

VII. CITATIONS

-
- [1] B. Schmidt and D. Redish, *Neuroscience: Navigation with a cognitive map*, Nature, 10.1038/nature12095 pp. 1476-4687 (2013).
- [2] J. O'Keefe and L. Nadel, *The Hippocampus as a cognitive map*, London, Oxford, (1978).
- [3] B. McNaughton, F. Battaglia, O. Jensen, E. Moser and M.-B. Moser, *Path integration and the neural basis of the 'cognitive map'*, Nat. Rev. Neurosci., 7, 663-678 (2006).
- [4] P. Best, A. White and A. Minai, Spatial processing in the brain: the activity of hippocampal place cells, *Annu. Rev. Neurosci.*, Vol. 24, pp. 459-86 (2001).
- [5] T. Davidson, F. Kloosterman and M. Wilson, *Hippocampal replay of extended experience*, Neuron Vol. 63, pp. 497-507 (2009).
- [6] B. Pfeiffer and D. Foster, *Hippocampal place-cell sequences depict future paths to remembered goals*, Nature (2013).
- [7] K. Louie and M. A. Wilson, *Temporally structured replay of awake hippocampal ensemble activity during rapid eye movement sleep*, Neuron 29, no. 1, pp. 145-56 (2001).
- [8] W. Skaggs, and B. McNaughton, *Replay of neuronal firing sequence in rat hippocampus during sleep following spatial experience*, Science 271, pp. 1870-1873 (1996).
- [9] M. Wilson and B. McNaughton, *Reactivation of hippocampal ensemble memories during sleep*, Science, Vol. 265, pp. 676-679 (1994).
- [10] D. Foster and M. Wilson, *Reverse replay of behavioural sequences in hippocampal place cells during the awake state*, Nature Vol. 440, pp. 680-683 (2006).
- [11] K. Diba and G. Buzsaki *Forward and reverse hippocampal place-cell sequences during ripples*, Nat. Neurosci., Vol. 10, pp. 1241-1242 (2007).
- [12] M. Hasselmo, *Temporally structured replay of neural activity in a model of entorhinal cortex, hippocampus and postsubiculum*, Eur J Neurosci 28(7), pp. 1301-1315 (2008).
- [13] M. Carr, S. Jadhav and L. Frank, *Hippocampal replay in the awake state: a potential substrate for memory consolidation and retrieval*, Nat Neurosci. Vol. 14, pp. 147-153 (2011).
- [14] A. Johnson and D. Redish, *Neural ensembles in CA3 transiently encode paths forward of the animal at a decision point*, J. Neurosci., Vol. 27, pp. 12176-12189 (2007).
- [15] E. Pastalkova, V. Itskov, A. Amarasingham and G. Buzsaki, *Internally Generated Cell Assembly Sequences in the Rat Hippocampus*, Science 321, p. 1322 (2008).
- [16] G. Dragoi and S. Tonegawa, *Preplay of future place cell sequences by hippocampal cellular assemblies*, Nature, Vol. 469(7330), pp. 397-401 (2011).
- [17] A. Tsao, M.-B. Moser and E. Moser, *Traces of Experience in the Lateral Entorhinal Cortex*, Curr. Biol., Vol. 23(5) pp. 399 - 405 (2013).
- [18] Hopfield, J., *Neurodynamics of mental exploration*, PNAS, Vol. 107(4), pp. 1648-1653, (2010).
- [19] M. E. Hasselmo, L. M. Giocomo, M. P. Brandon and M. Yoshida, *Cellular dynamical mechanisms for encoding the time and place of events along spatiotemporal trajectories in episodic memory*, Behav. Brain Res., Vol. 215(2), pp. 261-74 (2010).
- [20] G. Buzsaki, *Neural syntax: cell assemblies, synapsembles, and readers*, Neuron 68: 362-385 (2010).
- [21] E. Brown, L. Frank, D. Tang, M. Quirk and M. Wilson, *A statistical paradigm for neural spike train decoding applied to position prediction from ensemble firing patterns of rat hippocampal place cells*, J. Neurosci., 18: 7411-7425 (1998).
- [22] T. Jarsky, A. Roxin, W. Kath and N. Spruston, *Conditional dendritic spike propagation following distal synaptic activation of hippocampal CA1 pyramidal neurons*, Nat Neurosci 8, pp. 1667-1676 (2005).
- [23] Y. Katz, W. Kath, N. Spruston and M. Hasselmo, *Coincidence detection of place and temporal context in a network model of spiking hippocampal neurons*, PLoS Comput Biol 3: e234 (2007).
- [24] Dabaghian Y, Brandt VL, Frank LM (2014) Reconceiving the hippocampal map as a topological template, *eLife* 10.7554/eLife.03476.
- [25] Alvernhe, A., Sargolini, F., Poucet, B. (2012). Rats build and update topological representations through exploration. *Anim Cogn*, 15, 359-368.

- [26] Wu, X., Foster, D. (2014). Hippocampal Replay Captures the Unique Topological Structure of a Novel Environment, *J. of Neurosci.*, **34**, 6459-6469.
- [27] A. Samsonovich and B. McNaughton, *Path integration and cognitive mapping in a continuous attractor neural network model*, *J. Neurosci.*, 1997. 17(15): pp. 5900-20.
- [28] A. Gupta, M. van der Meer, D. Touretzky and A. Redish, *Hippocampal Replay Is Not a Simple Function of Experience*, *Neuron* 65, pp. 695-705 (2010).
- [29] J. Issa and K. Zhang, *Universal conditions for exact path integration in neural systems*, *PNAS* 109(17): 6716-6720 (2012).
- [30] S. P. Novikov, *Discrete connections and linear difference equations*, *Tr. Mat. Inst. Steklova*, 247(Geom. Topol. i Teor. Mnoz.): pp. 186–201 (2004).
- [31] Prasolov V. V. (2006). *Elements of combinatorial and differential topology*, Providence, R.I.: American Mathematical Society. xii, 331 pp.
- [32] Aleksandrov, P. S. (1965). *Elementary concepts of topology*, New York: F. Ungar Pub. Co. 63 pp.
- [33] G. E. Bredon, *Topology and geometry*, New York, Springer (1997).
- [34] B. A. Dubrovin, A. T. Fomenko and S. P. Novikov, *Modern geometry—methods and applications*, New York, Springer-Verlag (1992).
- [35] S. Sternberg, *Lectures on differential geometry*, New York: Chelsea (1964).
- [36] U. Eden, L. Frank, R. Barbieri, V. Solo and E. Brown, *Dynamic analysis of neural encoding by point process adaptive filtering* *Neural Comput.* 16, pp. 971-998 (2004).
- [37] Y. Dabaghian, F. Mémoli, L. Frank, G. Carlsson, *A Topological Paradigm for Hippocampal Spatial Map Formation Using Persistent Homology*, *PLoS Comput. Biol.*, 8(8): e1002581 (2012).
- [38] M. Arai, V. Brandt and Y. Dabaghian, *The Effects of Theta Precession on Spatial Learning and Simplicial Complex Dynamics in a Topological Model of the Hippocampal Spatial Map*, *PLoS Comput Biol* 10(6): e1003651 (2014).
- [39] A. Babichev, F. Memoli and Yu. Dabaghian (2015), *Combinatorics of Place Cell Coactivity and Hippocampal Maps*, in submission.
- [40] A. Georgopoulos, A. Schwartz and R. Kettner, *Neuronal population coding of movement direction*, *Science* 233: 1416-1419 (1986).
- [41] O. Tudusciuc and A. Nieder, *Neuronal population coding of continuous and discrete quantity in the primate posterior parietal cortex*, *PNAS* 104, pp. 14513-14518 (2007).
- [42] C. Huyck, *Overlapping cell assemblies from correlators*, *Neurocomputing*, 56, pp. 435-439 (2004).
- [43] E. Byrne and C. Huyck *Processing with cell assemblies*, *Neurocomputing* 74: 76-83 (2010).
- [44] N. Sigala, F. Gabbiani and N. Logothetis, *Visual Categorization and Object Representation in Monkeys and Humans*, *J. Cogn. Neurosci.* 14: 187-198 (2002).
- [45] R. Bogacz, *Optimal decision network with distributed representation*, *Neural Networks* 20: pp. 564-576 (2007).
- [46] T. Jahans-Price, T. Gorochofski, M. Wilson, M. Jones and R. Bogacz, *Computational modelling and analysis of hippocampal-prefrontal information coding during a spatial decision-making task*, *Front. Behav. Neurosci.* 8 (2014).
- [47] A. Maurer, S. Cowen, S. Burke, C. Barnes and B. McNaughton, *Organization of hippocampal cell assemblies based on theta phase precession*, *Hippocampus*, 16(9): pp. 785-94 (2006).
- [48] A. Gupta, M. van der Meer, D. Touretzky and A. Redish, *Segmentation of spatial experience by hippocampal theta sequences*, *Nat. Neurosci* 15, pp. 1032-1039 (2012).
- [49] C. Curto and V. Itskov, *Cell Groups Reveal Structure of Stimulus Space*, *PLoS Comput. Biol.* 4(10): e1000205 (2008).
- [50] G. Buzsaki, *Two-stage model of memory trace formation: A role for “noisy” brain states*. *Neuroscience* 31, pp. 551-570 (1989).
- [51] B. Broda, *Non-Abelian Stokes Theorem*, *Modern Nonlinear Optics, Part II*: John Wiley & Sons, Inc. pp. 429-468 (2002).
- [52] P. Poirazi, T. Brannon and B. Mel, *Arithmetic of Subthreshold Synaptic Summation in a Model CA1 Pyramidal Cell*, *Neuron* 37, pp. 977-987 (2003).
- [53] P. Poirazi, T. Brannon and B. Mel, *Pyramidal Neuron as Two-Layer Neural Network*, *Neuron* 37, pp. 989-999 (2003).
- [54] A. Wallach, D. Eytan, A. Gal, C. Zrenner and S. Marom, *Neuronal Response Clamp*, *Frontiers in Neuroengineering* 4 (2011).
- [55] P. Lienhardt, *N-Dimensional Generalized Combinatorial Maps and Cellular Quasi-Manifolds*, *Int. J. Comput.*

- Geometry Appl. 4(3):275-324 (1994).
- [56] L. Floriani, M. Mesmoudi, F. Morando and E. Puppo., *Non-manifold Decomposition in Arbitrary Dimensions*, in *Discrete Geometry for Computer Imagery*, A. Braquelaire, J.-O. Lachaud, and A. Vialard, Editors, Springer Berlin Heidelberg, pp. 69-80, (2002).
 - [57] Z. Chen, F. Kloosterman, E. Brown and M. Wilson, *Uncovering spatial topology represented by rat hippocampal population neuronal codes*, *J Comput Neurosci.* 33, pp. 227-255 (2012).
 - [58] Z. Chen, S. Gomperts, J. Yamamoto and M. Wilson, *Neural representation of spatial topology in the rodent hippocampus*, *Neural Comput* 26, pp. 1-39 (2014).
 - [59] L. Frank, E. Brown and G. Stanley, *Hippocampal and cortical place cell plasticity: implications for episodic memory*, *Hippocampus* 16, pp. 775-784 (2006).
 - [60] G. Dragoi and G. Buzsaki, *Temporal encoding of place sequences by hippocampal cell assemblies*, *Neuron* 50, pp. 145-157 (2006).
 - [61] R. Legenstein and W. Maass, *On the Classification Capability of Sign-Constrained Perceptrons*, *Neural Comput.* 20, pp. 288-309 (2007).
 - [62] J. Hopfield, *Neurons with graded response have collective computational properties like those of two-state neurons*, *PNAS* 81, pp. 3088-3092 (1984).